Investigations via Kinetics and Multivariate Linear Regression Models of the Mechanism and Origins of Regioselectivity in a Palladium-Catalyzed Aryne Annulation

Erin E. Plasek‡, Brylon N. Denman‡, Courtney C. Roberts*

University of Minnesota, Department of Chemistry, Minneapolis, MN 55455

Arynes, palladium catalysis, regioselectivity.

ABSTRACT: The synthetic potential of unsymmetrically substituted arynes is not yet fully realized due to regioselectivity issues. Although many models exist to predict the regioselectivity of arynes, these models do not hold for metal-mediated reactions. Previously, we reported a way to induce regioselectivity in a metal-catalyzed aryne annulation reaction by using bulky monodentate phosphine ligands. Reported herein is a mechanistic investigation into the operative catalytic cycle within this transformation. Additionally, the molecular parameters responsible for regioselectivity have been examined via LFERs and multivariate linear regression. This model shows the interdependence on both the steric and electronic properties of the aryne and the size of the phosphine ligand for regioselectivity.

Arynes are powerful building blocks for the synthesis of decorated arenes[1,2]. The highly reactive nature of arynes has been leveraged to make many value-added species.[3–7] Despite their success, the full synthetic potential of arynes is not yet realized due to regioselectivity limitations. Regioselectivity challenges can arise when unsymmetrically substituted arynes are utilized.[8–15] Additionally, these regioselectivity issues can be amplified in metal-mediated aryne reactions as now additional parameters contribute to regioinduction.[16–29] Exploring regioselectivity within metal-bound arynes is crucial to expanding their utility as some transformations can only occur through metal-mediated processes.[6,7] To enable access to the full synthetic potential of arynes, we aim to systematically explore the factors governing regioselectivity in metal-catalyzed arynes reactions.

The regioselectivity of free arynes (non-metal bound arynes) has been extensively studied which has resulted in the development of many selectivity models[8–15,30–38]. The *Aryne Distortion Model*, developed by Garg and Houk, is the most inclusive model as it accounts for the largest array of regioselectivity trends within free arynes.[8] This model correlates the level of distortion within the triple bond of the aryne to regioselectivity; where the larger angle is favored for nucleophilic attack. Utilizing this model has accounted for the highly selective nature of the arynes shown in **Figure 1a** due to their high degree of distortion.[9] Knowledge of the elements that

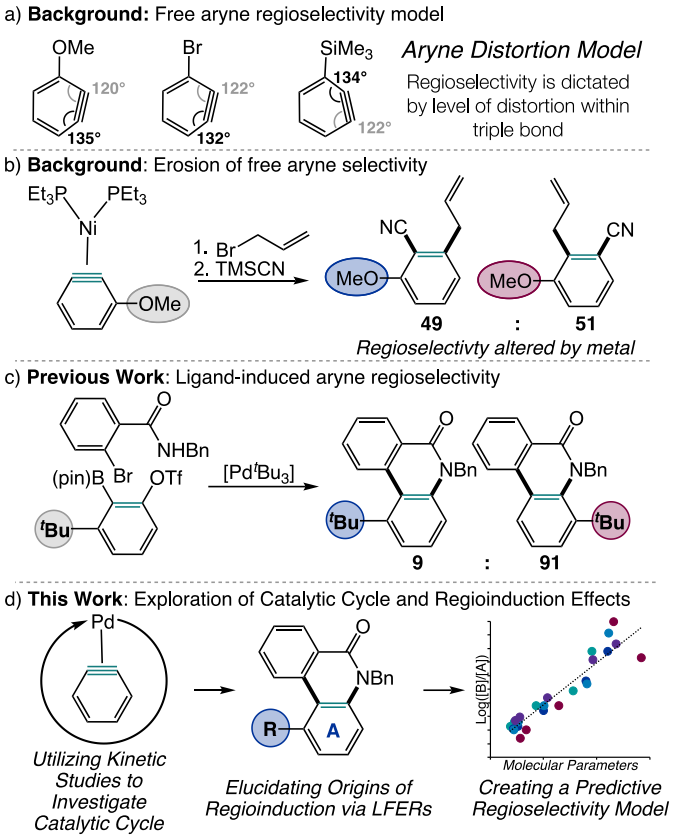

Figure 1 a) Free aryne regioselectivity model b) Erosion of free aryne selectivity c) ligand-induced regioselectivity d) exploration of catalytic cycle and regioinduction effects

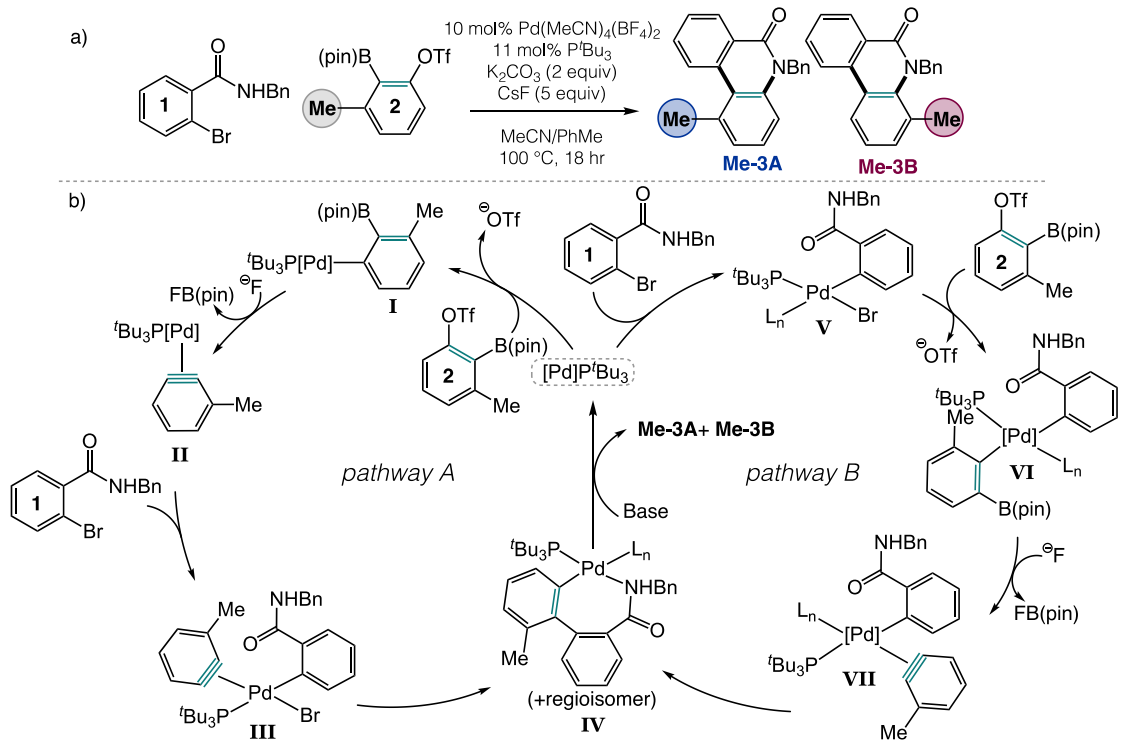

Figure 2 a) General scheme of annulation b) possible reaction pathways; L_n = solvent or bromide

influence selectivity has allowed for the successful enhancement and reversal of regioselectivity. For example, insight gained from the *Aryne Distortion Model* has allowed regioselectivity to be induced within arynes that exhibit poor inherent regioselectivity such as 3,4-pyridyne intermediates.[13,39,40]

In contrast, the factors influencing regioselectivity within metal-mediated aryne reactions are vastly understudied.[19] Unlike free arynes, there are no models for regioselectivity of arynes in the presence of metals. It is important to study metal-bound arynes because they do not follow the same trends as free arynes. In a report by Hosoya and coworkers, a *o*-methoxy benzyne nickel complex ligated with two triethylphosphine ligands reacts in an unselective manner (**Figure 1b)**.[16] This is in stark contrast to its free aryne counterpart which reacts in a highly selective manner due to its highly distorted triple bond (**Figure 1a**).[8] This suggests the same factors governing free aryne selectivity do not influence metal-bound aryne selectivity. A recent report from our lab disclosing the crystal structure and reactivity of an *o*-methoxy benzyne nickel complex ligated with an unsymmetric phosphinooxazoline (PHOX) ligand suggests the ligand environment contributes to regioinduction (**Figure 1b**).[20] These stoichiometric studies are in agreement with our previous catalytic studies.[17,41]

Previously, we reported a means of achieving regioselectivity in a palladium-catalyzed aryne annulation via catalyst-control.[17] By using an unsymmetrical ligand environment created by bulky monodentate phosphine ligands, such as tri-*tert*-butylphosphine (P^tBu_3), we were able to induce regioisomeric ratios of up to 9:91. (**Figure 1c**) Additionally, we have shown *o*-borylaryl triflates to be competent aryne precursors; however, the formation of metal-bound arynes with these precursors under catalytic conditions remains understudied. Thus, we seek to understand the mechanism behind aryne generation and functionalization within this palladium-catalyzed annulation. (**Figure 2a**) Herein we have elucidated the mechanism of this transformation through kinetic studies. Additionally, we aim to explicate the factors governing metal-bound aryne selectivity within our system. Linear free energy relationships (LFERs) and multivariate linear regression are utilized to explore the specific molecular parameters responsible for selectivity (**Figure 1c**). This will allow for a more systematic approach to be taken to improve regioselectivity as well as create a platform for future metal-catalyzed aryne reactions.

Results and Discussion

Possible Catalytic Cycles

To understand the mechanism of aryne formation and functionalization, the elementary steps of the catalytic cycle must be examined. This annulation was previously reported by Larock and coworkers.[42] In this report, two possible catalytic pathways were proposed using Kobayashi aryne precursors. Since we opted to utilize *o*-borylaryl triflates as aryne precursors we proposed two similar pathways accounting for the additional elementary steps required to generate an aryne (**Figure 2**). In pathway A, oxidative addition into aryl triflate **2** occurs first to generate **I**. This is then followed by activation/transmetallation of the boronic ester to produce a palladium-bound aryne intermediate **II**. After aryne formation, **II** can then undergo oxidative addition into **1** to generate **III**. Next, migratory insertion generates common intermediate **IV**. Reductive elimination then follows after deprotanation of the nitrogen to turn over the catalytic cycle and generate the phenanthridinone products (**Me-3A** and **Me-3B**). Pathway B is similar to pathway A, however, oxidative addition into the aryl bromide **1** occurs first to generate **V**. This is then followed by aryne formation via oxidative addition and transmetallation of **2** to generate **VII**. Next reductive elimination generates common intermediate **IV**. In pathway B, oxidative addition of the aryl triflate **2** must occur with a Pd(II) species to generate a Pd(IV) intermediate. Based on the insufficient oxidative

potential of **2** as well kinetic studies *vide infra*, we hypothesize that pathway A is most likely operative to avoid a Pd(IV) intermediate.

Kinetic Order of Substrates (1 and 2)

To elucidate which reaction pathway is operative, we investigated the turnover-limiting step by probing the kinetic order of both benzamide (**1**) and aryne precursor (**2**). From initial rates analysis, we observe a first order dependence of **2** (**Figure 3**). This suggests that **2** is involved in the turnover-limiting step. Initial rates analysis reveals a zero-order dependence of **1** (**Figure S10**). Since little correlation is observed between a change in concentration of **1** and reaction rate, we can conclude that **1** is not involved in the turnover-limiting step. Overall, this supports pathway A being the operative pathway since only **2** is involved the turnover-limiting step. If pathway B were operative, we would likely to see an increase in reaction rate at higher concentrations of **1** since oxidative addition of **1** would occur prior to the turnover-limiting step; however, this is not observed. This, in addition to the unlikelihood of a Pd(IV) intermediate, provides further support against pathway B. From these analyses, we hypothesize pathway A as the operative pathway.

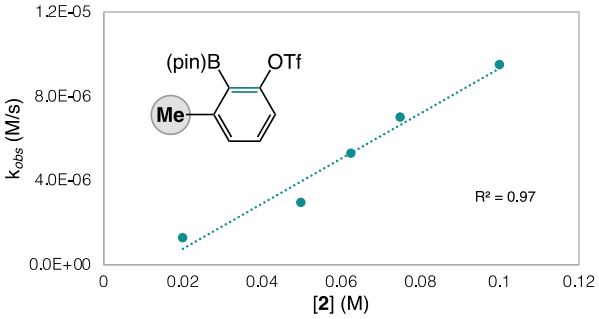

Figure 3 Initial rates analysis of aryne precursor (**2**) k_{obs} calculated based on method of initial rates measuring sum of regioisomers ([Me-3A] and [Me-3B]) via ^{1}H NMR spectroscopy with mesitylene as internal standard. Each point is an average of duplicated trials.

Kinetic Order of Catalyst

Initial rates studies were also conducted to obtain the kinetic order of the catalyst. Surprisingly, a nonlinear correlation was observed between catalyst loading and reaction rate (**Figure 4**). The fastest reaction rate occurred at 10 mol % loading of palladium which was also the optimal loading of catalyst previously reported. At lower loadings of catalyst (2.5 to 10 mol %) a positive linear correlation is observed (see **Figure S24**) suggesting that there is a 1st order dependence on the catalyst at lower palladium loadings. This is consistent with a monomeric palladium species in the turnover-limiting step. However, at higher concentrations of palladium (12.5 to 20 mol %), the rate of reaction slows and thus does not follow the 1st order dependence. Instead, a -2.3 order is obtained at higher catalyst loading (see **Figure S26**) which suggest that an off-cycle pathway is slowing the reaction. One possible explanation for this is that the palladium-bound aryne intermediate (**II**) could bind to another equivalent of catalyst (**Figure 4**).[43] This equilibrium would produce a non-integer rate order and account for the decreased rate. Overall, the study demonstrates a necessary consideration for catalysis involving aryne intermediates that has not previously been reported.

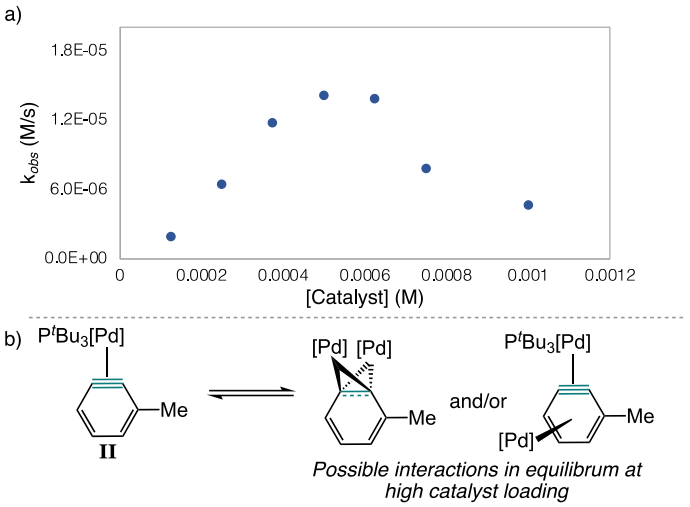

Figure 4 a) Initial rates analysis of catalyst b) proposed equilibrium at high catalyst loading. k_{obs} calculated based on method of initial rates measuring sum of regioisomers ([Me-3A] and [Me-3B]) via ^{1}H NMR spectroscopy with mesitylene as internal standard. Each point is an average of duplicated trials using 0.1 mmol (**1**) and 0.15 mmol (**2**).

Eyring Analysis

From initial rates analysis, **2** was determined to be involved in the turnover-limiting step. This means that either oxidative addition of the aryl triflate or transmetallation of the boronic ester contain the highest energy barrier of the catalytic cycle. To further elucidate the identity of the turnover-limiting step, Eyring analysis was performed to obtain the activation barriers.

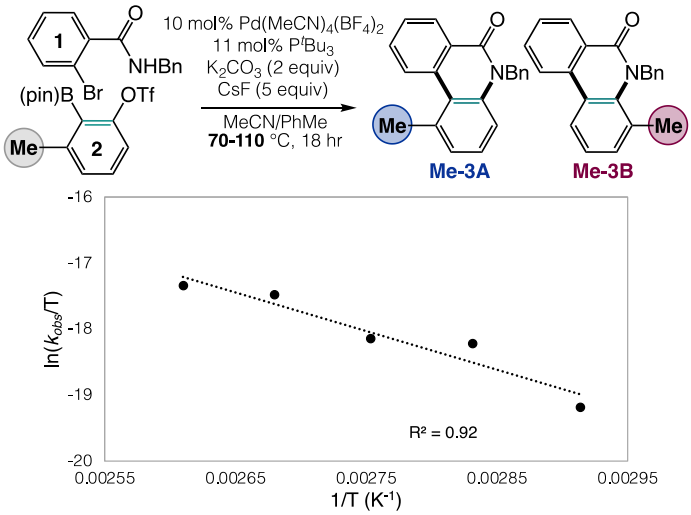

Figure 5 Eyring plot. k_{obs} calculated based on method of initial rates measuring sum of regioisomers ([Me-3A] and [Me-3B]) via ^{1}HNMR spectroscopy with mesitylene as internal standard. Each point is an average of duplicated trials using 0.1 mmol (**1**) and 0.15 mmol (**2**).

To construct the Eyring plot (**Figure 5**), initial rates were measured at varying temperatures (70 -110 °C). From the slope and intercept of the Eyring plot the following activation parameters were obtained: $\Delta G^{\ddagger}$ = 30.7 kcal/mol, $\Delta H^{\ddagger}$ = 11.7 kcal/mol and $\Delta S^{\ddagger}$ = −50.9 cal/(mol·K). The highest energetic barrier to generate a metal-bound aryne in this system is 30.7 kcal/mol. This value is significantly larger than previously

reported values for oxidative addition of an aryl triflate with palladium.[44,45] This suggests that transmetallation is likely the turnover-limiting step. Additionally, since the aryl triflate outcompetes the aryl bromide to undergo oxidative addition first in the catalytic cycle, transmetallation is further supported as the turnover-limiting step.

Measuring Ligand Steric Contribution through Charton Analysis

Previously, we performed Charton analysis by varying the size of the aryne substituent (Me, Et, ^{i}Pr, and ^{t}Bu) and observing changes in regioselectivity.[41,46,47] From this, we discovered that the aryne steric environment impacted selectivity. Additionally, we found the slope (ψ) of the Charton plot differed greatly between symmetric and unsymmetric ligand environments.[18] This indicated to us that the ligand's identity also impacts regioselectivity. To systematically study the ligand's contribution to regioselectivity, we performed Charton analyses using the same set of previously studied substituted aryne precursors (Me, Et, ^{i}Pr, and ^{t}Bu) with a library of monodentate phosphine ligands that vary in their steric profile ($PtBu_3$, P(o-tol)$_3$, CataCXium® A, PCy_3, PPh_3, PPh_2Me, and PEt_3). For this study, we implemented Buchwald-style palladacycle precatalysts to rigorously ensure an unsymmetrical ligand environment via a 1:1 ratio between palladium and the monodentate phosphine ligand (**Figure 6a**). The Charton plot of each ligand displayed high linearity (R^2 = 0.96 to 0.99), but the slope or sensitivity (ψ) of each line was dependent on the ligand (ψ = 0.35 to 2.07) (**Figure 6b**). This corroborates that the identity of the ligand does influence regioselectivity. If the ligand did not impact the regioselectivity, the slope of the Charton plots should remain consistent across all ligands.

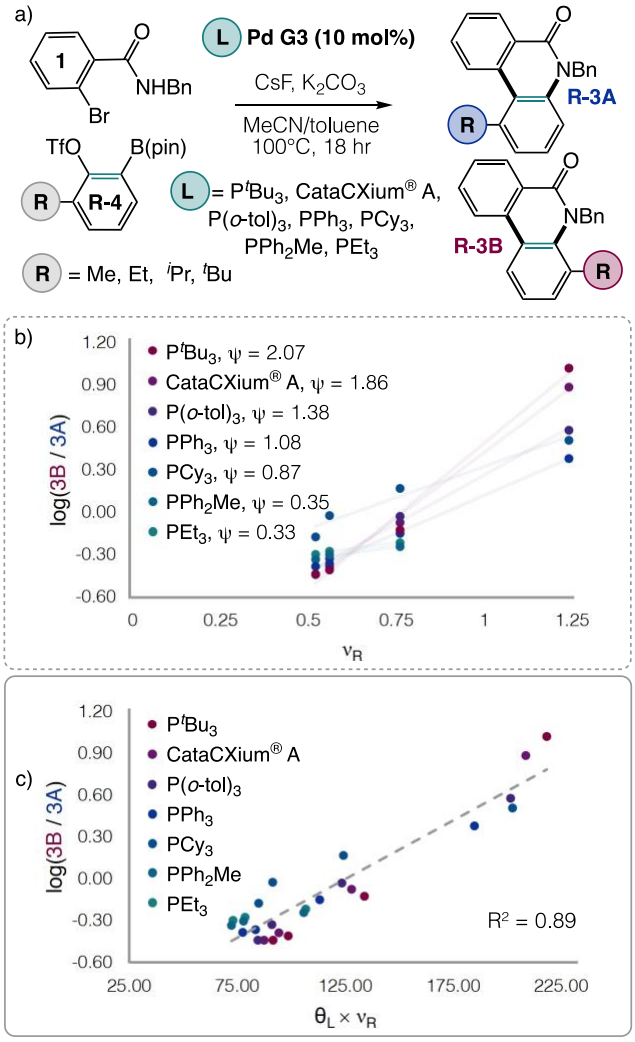

Figure 6 a) Aryne annulation conditions using a series of alkyl-substituted arynes and a variety of phosphine-ligated Buchwald-style palladacycle precatalysts. b) Charton analysis using each phosphine ligand individually. c) LFER model relating the regioselectivity of the aryne annulation to the product of the ligand's cone angle and the Charton value of the aryne substituent.

Using the Charton value (ν) of the aryne substituent as a singular molecular descriptor resulted in an "underfit" linear relationship. This indicates that multiple reactions with the same molecular descriptor gave rise to various selectivity outcomes (**Figure 6b)**. It was evident that incorporation of a ligand molecular descriptor was necessary for a better fit. We observed that the Charton relationships with the greatest sensitivities (ψ) were generally correlated with bulkier ligands measured by minimum cone angle (θ).[48] The changes in slope indicated that the ligand descriptor should serve as a multiplying factor, rather than additive. Therefore, the logarithmic value of the regioisomeric ratio (log(3B/3A)) was plotted against the ligand cone angle multiplied by the aryne Charton value ($\theta_L \times \nu_R$), resulting in high linearity (R^2 = 0.89) (**Figure 6c**). The linear best fit of these data can be described by the following equation:

$$\log\left(\frac{3B}{3A}\right) = 0.01(\theta_L \times \nu_R) - 1.06 \quad (1)$$

This demonstrates that ligand steric encumbrance amplifies the steric effects of the aryne substituent on regioselectivity. Thus, a combination of increased sterics of the aryne (measured via ν) and ligand (measured via θ) will lead to greater regioselectivity for regioisomer B.

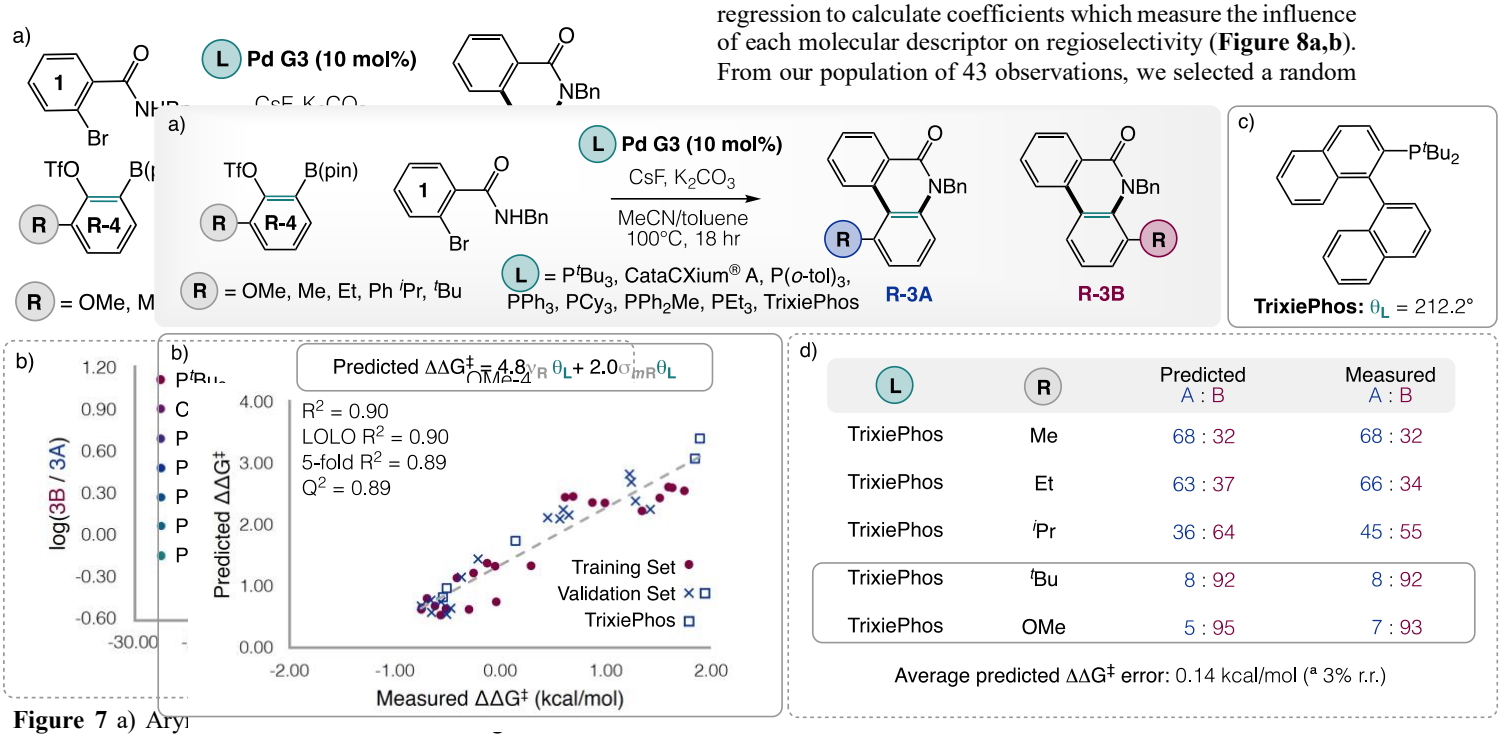

L	R	Predicted A : B	Measured A : B
TrixiePhos	Me	68 : 32	68 : 32
TrixiePhos	Et	63 : 37	66 : 34
TrixiePhos	iPr	36 : 64	45 : 55
TrixiePhos	tBu	8 : 92	8 : 92
TrixiePhos	OMe	5 : 95	7 : 93

Figure 7 a) Aryne annulation conditions using a series of phosphine-ligated Buchwald-style palladacycle precatalysts and a variety of arynes with similarly sized but electronically differentiated substituents. b) LFER model relating the regioselectivity of the aryne annulation to the product of the ligand's cone angle and the σm parameter of the aryne substituent.

Figure 8 a) Aryne annulation conditions using a series of phosphine-ligated Buchwald-style palladacycle precatalysts and arynes with substituents of various size and electronics. b) Multivariate linear regression correlating regioselectivity of the aryne annulation to a combination of ligand cone angle and the Hammet and Charton parameters associated with the aryne substituent. c) Experimental regioselectivity using TrixiePhos ligand vs. the regioselectivity predicted by multivariate linear

Electronic influences of aryne substituent

In order to decouple steric and electronic effects on regioselectivity, we performed similar analyses with a subset of "isosteric" arynes with varied electronics (**OMe-4**, **Me-4**, **Et-4**, and **Ph-4**) (**Figure 7a**). From these studies, we discovered a linear relationship between regioselectivity and the ligand cone angle multiplied by the Hammett parameter of the aryne substituent ($\theta_L \times \sigma_m$) (**Figure 7b**).[49] The linear best fit of these data can be described by the following equation:

$$\log\left(\frac{3B}{3A}\right) = 0.04(\theta_L \times \sigma_{mR}) + 0.08 \qquad (2)$$

Using σ_m allows us to directly probe the partial charge at one terminus of the triple bond. It should be noted that plotting σ_p in the same manner does not result in a linear relationship (See **Figure S35**). We believe this is because σ_p incorporates resonance effects that are unlikely to occur in an aryne system as a strained cyclic allene would be produced. Additionally, σ_p does not directly probe either terminus of the triple bond. Overall, the linear relationship in **Figure 7b** and **equation 2** indicates that more inductively withdrawing substituents (measured via σ_m) lead to greater regioselectivity for regioisomer B.

Using multivariate linear regression to account for regioselectivity trends

Having discovered the individual components of regioselectivity (ν, σ_m, and θ) we next sought to combine them together into one comprehensive linear equation to account for regioselectivity ($\Delta\Delta G^{\ddagger}$). We performed a multivariate linear regression to calculate coefficients which measure the influence of each molecular descriptor on regioselectivity (**Figure 8a,b**). From our population of 43 observations, we selected a random sample of 22 to serve as our training set (See **Figure S33**) in the linear regression, and the remaining 21 observations served as the validation set for the calculated coefficients (See **Figure S34**). Linear regression using normalized molecular parameters yields the following equation:

$$\Delta\Delta G^{\ddagger} = 4.8\nu_R\theta_L + 2.0\sigma_{mR}\theta_L \qquad (3)$$

The calculated coefficient for the steric term (ν) is greater than that of the electronic term, which indicates that steric encumbrance has the greatest contribution to regioselectivity.

Upon plotting the training and validation sets we observed a highly linear relationship ($R^2 = 0.90$) (**Figure 8b**). Additionally, cross-validation methods like leave one ligand set out (LOLO), 5-fold cross-validation, and Q^2 display high linearity. This indicates the reliability of the molecular parameters with their calculated coefficients to account for regioselectivity.

With the goal of maximizing regioselectivity, we next sought to exploit the limits of our linear equation. Based on the equation we can enhance regioselectivity most by increasing the cone angle of the ligand (θ_L) as it serves to amplify both steric and electronic terms of the aryne. Based on this observation, we identified TrixiePhos as the optimal ligand for regioinduction due to its large cone angle (θ = 212.2°).[48] In accordance with our previous analyses, we observe highest regioselectivity with our most sterically hindered aryne (tBu-4) and our most

inductively withdrawing aryne (OMe-4) when TrixiePhos is employed as the ligand.

As TrixiePhos was not included in the linear regression, we sought to determine if it would follow the linear relationship as described by equation 3. The average $\Delta\Delta G^{\ddagger}$ error between the predicted and measured regioselectivity values using TrixiePhos was 0.14 kcal/mol, which is associated with a small 3% average error in regioisomeric ratio (**Figure 8c,d**). This indicates that our linear equation does account for regioselectivity trends when using TrixiePhos.

Conclusion

In summary, we have elucidated the turnover-limiting step of this metal-catalyzed aryne annulation through kinetic analysis. Initial rate studies reveal that only aryne precursor and palladium catalyst are involved in the turnover-limiting step. Based on the $\Delta G^{\ddagger}$ obtained from Eyring analysis, we hypothesize that the turnover-limiting step is the transmetallation of the aryne precursor. LFERs and multivariate linear regression reveal the influence of steric and electronic effects on the regioselectivity of this metal-bound aryne annulation. Additionally, we have used these findings to optimize regioinduction using TrixiePhos. Identifying the individual contributors of aryne and ligand demystifies aryne regioselectivity and will provide a platform for enhancing the regioselectivity of other metal-catalyzed aryne reactions. We are currently studying the regioselectivity of other metal-mediated aryne reactions in a similar manner to gauge the generality of these regioselectivity-determining parameters.

ASSOCIATED CONTENT

Supporting Information

The Supporting Information is available free of charge on the ACS Publications website.

Experimental details and characterization (PDF)

AUTHOR INFORMATION

Corresponding Author

* ccrob@umn.edu

Author Contributions

The manuscript was written through contributions of all authors. ‡These authors contributed equally.

Funding Sources

The NIH R35GM146957 is acknowledged as the primary funding source. We also thank the UMN Newman and Lillian Bortnick Excellence Fellowship (E.E.P.), UMN Doctoral Dissertation Fellowship (E.E.P. and B.N.D), Robert and Jill DeMaster Departmental Fourth Year Excellence Fellowship (B.N.D.) Amgen Young Investigator Award (C.C.R.), 3M-Alumni Professorship (C.C.R.), and McKnight Land-Grant Professorship (C.C.R.) for support. Instrumentation funding is acknowledged as well: NIH NMR Instrumentation (S10OD011952), NSF MS Instrumentation (CHE-1336940), NSF MRI Grant for Crystallography (1229400).

ACKNOWLEDGMENT

We thank the T. Hoye lab for access to IR instrumentation. We thank A. Umanzor and S. Neufeldt for helpful discussions.

REFERENCES

(1) Shi, J.; Li, L.; Li, Y. O-Silylaryl Triflates: A Journey of Kobayashi Aryne Precursors. *Chem. Rev.* **2021**, *121* (7), 3892–4044. https://doi.org/10.1021/acs.chemrev.0c01011.

(2) Tadross, P. M.; Stoltz, B. M. A Comprehensive History of Arynes in Natural Product Total Synthesis. *Chem. Rev.* **2012**, *112* (6), 3550–3577. https://doi.org/10.1021/cr200478h.

(3) Kamikawa, K. Asymmetric Reactions Involving Aryne Intermediates. *Nat. Rev. Chem.* **2023**, *7* (7), 496–510. https://doi.org/10.1038/s41570-023-00485-y.

(4) Wenk, H. H.; Winkler, M.; Sander, W. One Century of Aryne Chemistry. *Angew. Chem. Int. Ed.* **2003**, *42* (5), 502–528. https://doi.org/10.1002/anie.200390151.

(5) Takikawa, H.; Nishii, A.; Sakai, T.; Suzuki, K. Aryne-Based Strategy in the Total Synthesis of Naturally Occurring Polycyclic Compounds. *Chem. Soc. Rev.* **2018**, *47* (21), 8030–8056. https://doi.org/10.1039/C8CS00350E.

(6) Dhokale, R. A.; Mhaske, S. B. Transition-Metal-Catalyzed Reactions Involving Arynes. *Synthesis* **2018**, *50* (01), 1–16. https://doi.org/10.1055/s-0036-1589517.

(7) Feng, M.; Jiang, X. Reactions of Arynes Involving Transition-Metal Catalysis. *Synthesis* **2017**, *49* (19), 4414–4433. https://doi.org/10.1055/s-0036-1589094.

(8) Medina, J. M.; Mackey, J. L.; Garg, N. K.; Houk, K. N. The Role of Aryne Distortions, Steric Effects, and Charges in Regioselectivities of Aryne Reactions. *J. Am. Chem. Soc.* **2014**, *136* (44), 15798–15805. https://doi.org/10.1021/ja5099935.

(9) Bronner, S. M.; Mackey, J. L.; Houk, K. N.; Garg, N. K. Steric Effects Compete with Aryne Distortion To Control Regioselectivities of Nucleophilic Additions to 3-Silylarynes. *J. Am. Chem. Soc.* **2012**, *134* (34), 13966–13969. https://doi.org/10.1021/ja306723r.

(10) Cheong, P. H.-Y.; Paton, R. S.; Bronner, S. M.; Im, G.-Y. J.; Garg, N. K.; Houk, K. N. Indolyne and Aryne Distortions and Nucleophilic Regioselectivites. *J. Am. Chem. Soc.* **2010**, *132* (4), 1267–1269. https://doi.org/10.1021/ja9098643.

(11) Anthony, S. M.; Wonilowicz, L. G.; McVeigh, M. S.; Garg, N. K. Leveraging Fleeting Strained Intermediates to Access Complex Scaffolds. *JACS Au* **2021**, *1* (7), 897–912. https://doi.org/10.1021/jacsau.1c00214.

(12) Garr, A. N.; Luo, D.; Brown, N.; Cramer, C. J.; Buszek, K. R.; VanderVelde, D. Experimental and Theoretical Investigations into the Unusual Regioselectivity of 4,5-, 5,6-, and 6,7-Indole Aryne Cycloadditions. *Org. Lett.* **2010**, *12* (1), 96–99. https://doi.org/10.1021/ol902415s.

(13) Goetz, A. E.; Garg, N. K. Regioselective Reactions of 3,4-Pyridynes Enabled by the Aryne Distortion Model. *Nat. Chem.* **2013**, *5* (1), 54–60. https://doi.org/10.1038/nchem.1504.

(14) Bronner, S. M.; Goetz, A. E.; Garg, N. K. Overturning Indolyne Regioselectivities and Synthesis of Indolactam V. *J. Am. Chem. Soc.* **2011**, *133* (11), 3832–3835. https://doi.org/10.1021/ja200437g.

(15) Im, G.-Y. J.; Bronner, S. M.; Goetz, A. E.; Paton, R. S.; Cheong, P. H.-Y.; Houk, K. N.; Garg, N. K. Indolyne Experimental and Computational Studies: Synthetic Applications and Origins of Selectivities of Nucleophilic Additions. *J. Am. Chem. Soc.* **2010**, *132* (50), 17933–17944. https://doi.org/10.1021/ja1086485.

(16) Sumida, Y.; Sumida, T.; Hashizume, D.; Hosoya, T. Preparation of Aryne–Nickel Complexes from Ortho-Borylaryl Triflates. *Org. Lett.* **2016**, *18* (21), 5600–5603. https://doi.org/10.1021/acs.orglett.6b02831.

(17) Denman, B. N.; Plasek, E. E.; Roberts, C. C. Ligand-Induced Regioselectivity in Metal-Catalyzed Aryne Reactions Using Borylaryl Triflates as Aryne Precursors. *Organometallics* **2023**, *42* (10), 859–864. https://doi.org/10.1021/acs.organomet.3c00103.

(18) Plasek, E. E.; Denman, B. N.; Roberts, C. C. Insights into the Regioselectivity of Metal-Catalyzed Aryne Reactions. *Synlett* **2024**, *35* (07), 747–752. https://doi.org/10.1055/s-0042-1751487.

(19) Humke, J. N.; Belli, R. G.; Plasek, E. E.; Kargbo, S. S.; Ansel, A. Q.; Roberts, C. C. Nickel Binding Enables Isolation and Reactivity of Previously Inaccessible 7-Aza-2,3-Indolynes. *Science* **2024**, *384* (6694), 408–414. https://doi.org/10.1126/science.adi1606.

(20) Umanzor, A.; Garcia, N. A.; Roberts, C. C. Ligand-Controlled Regioinduction in a PHOX-Ni Aryne Complex. *ACS Org. Inorg. Au* **2024**, *4* (1), 97–101. https://doi.org/10.1021/acsorginorgau.3c00046.

(21) Huang, X.; Sha, F.; Tong, J. Facile and Efficient Synthesis of Hydrophenanthren-1(2H)-Ones and Naphtho[2,1-c]Furan-3(1H)-Ones by a Palladium-Catalyzed Aryne Annulation Strategy. *Adv. Synth. Catal.* **2010**, *352* (2–3), 379–385. https://doi.org/10.1002/adsc.200900703.

(22) Lin, Y.; Wu, L.; Huang, X. Palladium-Catalyzed [3+2] Cycloaddition Reaction of (Diarylmethylene)Cyclopropa[b]Naphthalenes with Arynes: An Efficient Synthesis of 11-(Diarylmethylene)-11H-Benzo[b]Fluorenes. *Eur. J. Org. Chem.* **2011**, *2011* (16), 2993–3000. https://doi.org/10.1002/ejoc.201100035.

(23) Li, R.-J.; Pi, S.-F.; Liang, Y.; Wang, Z.-Q.; Song, R.-J.; Chen, G.-X.; Li, J.-H. Palladium-Catalyzed Annulations of Arynes with 2-(2-Iodophenoxy)-1-Substituted Ethanones. *Chem. Commun.* **2009**, *46* (43), 8183–8185. https://doi.org/10.1039/C0CC02720K.

(24) Tang, C.-Y.; Wu, X.-Y.; Sha, F.; Zhang, F.; Li, H. Pd-Catalyzed Assembly of Phenanthridines from Aryl Ketone O-Acetyloximes and Arynes through C–H Bond Activation. *Tetrahedron Lett.* **2014**, *55* (5), 1036–1039. https://doi.org/10.1016/j.tetlet.2013.12.075.

(25) Yoshida, H.; Honda, Y.; Shirakawa, E.; Hiyama, T. Palladium–Iminophosphine-Catalysed Carbostannylation of Arynes: Synthesis of Ortho-Substituted Arylstannanes. *Chem. Commun.* **2001**, *0* (18), 1880–1881. https://doi.org/10.1039/B103745P.

(26) Henderson, J. L.; Edwards, A. S.; Greaney, M. F. Biaryl Synthesis via Palladium-Catalyzed Aryne Multicomponent Coupling. *Org. Lett.* **2007**, *9* (26), 5589–5592. https://doi.org/10.1021/ol702584t.

(27) Jayanth, T. T.; Jeganmohan, M.; Cheng, C.-H. Highly Efficient Route to O-Allylbiaryls via Palladium-Catalyzed Three-Component Coupling of Benzynes, Allylic Halides, and Aryl Organometallic Reagents. *Org. Lett.* **2005**, *7* (14), 2921–2924. https://doi.org/10.1021/ol050859r.

(28) Jeganmohan, M.; Bhuvaneswari, S.; Cheng, C.-H. A Cooperative Copper- and Palladium-Catalyzed Three-Component Coupling of Benzynes, Allylic Epoxides, and Terminal Alkynes. *Angew. Chem. Int. Ed.* **2009**, *48* (2), 391–394. https://doi.org/10.1002/anie.200804873.

(29) Jeganmohan, M.; Cheng, C.-H. Substituted 1-Allyl-2-Allenylbenzenes via Palladium-Catalyzed Allylallenylation of Benzyne Derivatives. *Synthesis* **2005**, *2005* (10), 1693–1697. https://doi.org/10.1055/s-2005-869966.

(30) Goetz, A. E.; Bronner, S. M.; Cisneros, J. D.; Melamed, J. M.; Paton, R. S.; Houk, K. N.; Garg, N. K. An Efficient Computational Model to Predict the Synthetic Utility of Heterocyclic Arynes. *Angew. Chem. Int. Ed. 51* (11), 2758–2762. https://doi.org/10.1002/anie.201108863.

(31) Picazo, E.; Houk, K. N.; Garg, N. K. Computational Predictions of Substituted Benzyne and Indolyne Regioselectivities. *Tetrahedron Lett.* **2015**, *56* (23), 3511–3514. https://doi.org/10.1016/j.tetlet.2015.01.022.

(32) Goetz, A. E.; Garg, N. K. Enabling the Use of Heterocyclic Arynes in Chemical Synthesis. *J. Org. Chem.* **2014**, *79* (3), 846–851. https://doi.org/10.1021/jo402723e.

(33) Liu, Z.; Larock, R. C. Facile N-Arylation of Amines and Sulfonamides and O-Arylation of Phenols and Arenecarboxylic Acids. *J. Org. Chem.* **2006**, *71* (8), 3198–3209. https://doi.org/10.1021/jo0602221.

(34) Tadross, P. M.; Gilmore, C. D.; Bugga, P.; Virgil, S. C.; Stoltz, B. M. Regioselective Reactions of Highly Substituted Arynes. *Org. Lett.* **2010**, *12* (6), 1224–1227. https://doi.org/10.1021/ol1000796.

(35) Yoshida, H.; Sugiura, S.; Kunai, A. Facile Synthesis of N-Alkyl-N'-Arylimidazolium Salts via Addition of Imidazoles to Arynes. *Org. Lett.* **2002**, *4* (16), 2767–2769. https://doi.org/10.1021/ol0262845.

(36) Buszek, K. R.; Luo, D.; Kondrashov, M.; Brown, N.; VanderVelde, D. Indole-Derived Arynes and Their Diels−Alder Reactivity with Furans. *Org. Lett.* **2007**, *9* (21), 4135–4137. https://doi.org/10.1021/ol701595n.

(37) Takagi, A.; Ikawa, T.; Saito, K.; Masuda, S.; Ito, T.; Akai, S. Ortho-Selective Nucleophilic Addition of Amines to 3-Borylbenzynes: Synthesis of Multisubstituted Anilines by the Triple Role of the Boryl Group. *Org. Biomol. Chem.* **2013**, *11* (46), 8145–8150. https://doi.org/10.1039/C3OB41787E.

(38) Anthony, S. M.; Tona, V.; Zou, Y.; Morrill, L. A.; Billingsley, J. M.; Lim, M.; Tang, Y.; Houk, K. N.; Garg, N. K. Total Synthesis of (−)-Strictosidine and Interception of Aryne Natural Product Derivatives "Strictosidyne" and "Strictosamidyne." *J. Am. Chem. Soc.* **2021**, *143* (19), 7471–7479. https://doi.org/10.1021/jacs.1c02004.

(39) E. Goetz, A.; K. Shah, T.; K. Garg, N. Pyridynes and Indolynes as Building Blocks for Functionalized Heterocycles and Natural Products. *Chem. Commun.* **2015**, *51* (1), 34–45. https://doi.org/10.1039/C4CC06445C.

(40) Heinz, B.; Djukanovic, D.; Filipponi, P.; Martin, B.; Karaghiosoff, K.; Knochel, P. Regioselective Difunctionalization of Pyridines via 3,4-Pyridynes.

Chem. Sci. **2021**, *12* (17), 6143–6147. https://doi.org/10.1039/D1SC01208H.

(41) Plasek, E. E.; Denman, B. N.; Roberts, C. C. Insights into the Regioselectivity of Metal-Catalyzed Aryne Reactions. *Synlett* **2024**, *35* (07), 747–752. https://doi.org/10.1055/s-0042-1751487.

(42) Lu, C.; Dubrovskiy, A. V.; Larock, R. C. Palladium-Catalyzed Annulation of Arynes by o-Halobenzamides: Synthesis of Phenanthridinones. *J. Org. Chem.* **2012**, *77* (19), 8648–8656. https://doi.org/10.1021/jo3016192.

(43) Bennett, M. A.; Schwemlein, H. P. Metal Complexes of Small Cycloalkynes and Arynes. *Angew. Chem. Int. Ed. Engl.* **1989**, *28* (10), 1296–1320. https://doi.org/10.1002/anie.198912961.

(44) Lu, J.; Donnecke, S.; Paci, I.; Leitch, D. C. A Reactivity Model for Oxidative Addition to Palladium Enables Quantitative Predictions for Catalytic Cross-Coupling Reactions. *Chem. Sci.* **2022**, *13* (12), 3477–3488. https://doi.org/10.1039/D2SC00174H.

(45) Schoenebeck, F.; Houk, K. N. Ligand-Controlled Regioselectivity in Palladium-Catalyzed Cross Coupling Reactions. *J. Am. Chem. Soc.* **2010**, *132* (8), 2496–2497. https://doi.org/10.1021/ja9077528.

(46) Sigman, M. S.; Miller, J. J. Examination of the Role of Taft-Type Steric Parameters in Asymmetric Catalysis. *J. Org. Chem.* **2009**, *74* (20), 7633–7643. https://doi.org/10.1021/jo901698t.

(47) Charton, M. Steric Effects. I. Esterification and Acid-Catalyzed Hydrolysis of Esters. *J. Am. Chem. Soc.* **1975**, *97* (6), 1552–1556. https://doi.org/10.1021/ja00839a047.

(48) Gensch, T.; dos Passos Gomes, G.; Friederich, P.; Peters, E.; Gaudin, T.; Pollice, R.; Jorner, K.; Nigam, A.; Lindner-D'Addario, M.; Sigman, M. S.; Aspuru-Guzik, A. A Comprehensive Discovery Platform for Organophosphorus Ligands for Catalysis. *J. Am. Chem. Soc.* **2022**, *144* (3), 1205–1217. https://doi.org/10.1021/jacs.1c09718.

(49) Hansch, Corwin.; Leo, A.; Taft, R. W. A Survey of Hammett Substituent Constants and Resonance and Field Parameters. *Chem. Rev.* **1991**, *91* (2), 165–195. https://doi.org/10.1021/cr00002a004.